Mechanics of Advanced Composite Structures 10 (2023) 111 – 122

Semnan University

Mechanics of Advanced Composite Structures

journal homepage: http://MACS.journals.semnan.ac.ir

Low-Velocity Impact Behavior of Foam Core Sandwich Panels with Different Face Sheet Layers: Numerical and Experimental Study

M. A. Torabizadeh [a*], A. Fereidoon [b]

[a] *Department of Industrial, University of Applied Science and Engineering, Mashhad, 91379-33435, Iran*
[b] *Faculty of Mechanical Engineering, Semnan University, Semnan, 35131-19111, Iran*

KEYWORDS

Finite element model;
Low-velocity impact;
Sandwich panel;
Aluminum foam core;
Composite.

ABSTRACT

In this paper, some impact properties including maximum impact force, maximum displacement, specific absorbed energy, and failure mode of composite sandwich panels with aluminum foam core and different skin layers were investigated both numerically and experimentally. To compare the effect of different types of skin layers, in addition to the conventional aluminum layer, glass/epoxy composite with cross-ply and quasi-isotropic layouts was also employed. The experimental low-velocity impact tests were applied using a drop-weight device. All experimental tests were carried out based on the ASTM D7136. The finite element software, ABAQUS/Explicit, was employed to simulate the drop weight impact test of foam sandwiched composite. The finite element model was evaluated by comparing outputs between experimental results and the numerical simulation. Results showed that type of the face sheets and the fiber alignment in the composite surfaces significantly affected the impact behavior such as maximum impact force, failure mode, and absorbed energy. Based on the output results, the composite sheets with a quasi-isotropic skin layer had the highest specific absorbed energy. Moreover, in numerical results, the destruction area indicated more symmetry compared to the experimental ones. Also, the penetration depths of the impactor were completely dependent on the stacking sequence and type of top layer.

1. Introduction

Currently, sandwich composite sheets have found specific applications in the automotive, military, and aerospace fields. To decline the weight of the structure, the use of air-filled pores (or other neutral gases) to form a porous foam has received increasing attention. Numerous metals such as aluminum, copper, nickel, lead, zinc, magnesium, and titanium have foam ability properties through various processes. Among them, Al has gained huge attention due to its lightweight, low melting point, high specific stiffness, proper corrosion resistance, high strength, excellent energy absorption capacity, recyclability and possibility to be produced in homogenous and isotropic network structures. However, internal defects due to the impact loads and the declined residual resistance have remained among the main concerns [1].

The issue of the impact design can be addressed in two ways. Experimental approaches require several experiments under various environmental conditions, loading, and geometry; and the simulation approaches use finite element methods which require powerful hardware and software. Numerous tests are required to experimentally assess the effect of various parameters on material behavior. Numerical simulations can be also employed to achieve more accurate results with fewer experiments which can decrement the costs and time required for the design of the structure.

Mohmmed et al. [2] experimentally and numerically (finite element) investigated the composite sheets under the low-velocity impact (LVI). They also studied the influence of the fiber angles on the impact behavior of the materials which indicated a proper agreement between the

* Corresponding author. Tel.: +98-9155093689; Fax: +98-5138552304
E-mail address: torabizadeh@uast.ac.ir

DOI: 10.22075/macs.2022.27336.1407
Received 2022-05-30; Received in revised form 2022-09-19; Accepted 2022-10-17.

two methods. Bozkurt et al. [3] used ABAQUS/Explicit software to simulate the impact behavior of composites under dropping weight. Sun et al. [4] examined memory alloys of glass/epoxy under LVI with various energy levels. In addition to the agreement between the experimental and numerical results, they indicated that matrix cracking and delamination are the main failure modes at low energies, while fiber failure was the major type of sheet destruction at high energy levels. The effect of the layup on the LVI failure of composite sheets was addressed by Riccio et al. [5] using finite elements as implemented in ABACUS. Finite element modeling of composite pinned joints under impact load was the subject of a study by Gou et al. [6]. In another study, Soydan et al. [7] modeled (finite element, ANSYS) the collision of the bullet to multilayer guards and compared the results with experimental findings which indicated a proper consistency. Ahmad et al. [8] studied carbon composite sheets with perpendicular layup both experimentally and numerically. They also found that the use of shell elements will lead to better and more accurate results as compared to solid elements. Three-point bending of the sandwich composite with a metallic top layer along with a glass/epoxy composite layer and organic adhesives was the subject of a study by Wang et al. [9]. They reported an improvement in the performance of such sheets compared to conventional sandwich sheets and optimized the production parameters. Liu et al. [10] simulated high-velocity impact on kevlar/epoxy composite sheets using finite element software and confirmed them by their comparison with experimental results, which showed acceptable consistency. A numerical and experimental study of the effects of high-velocity impact on a composite with various layup and impactor geometries was addressed by Ciu et al. [11]. A good agreement was observed between the two methods. A numerical model was used to determine the impact velocity, impact load, and failure mode. Numerical modeling of high-velocity impact on ceramic composite was performed using AUTODIN finite element software and the results were compared with experimental findings of other researchers by Subramani and Kanna [12]. The best composite layup was proposed for optimal performance under impact load. Safarabadi et al. [13] presented a high-velocity numerical model of impact using Abaqus software and Matzenmiller theory for hybrid and non-hybrid polymer composite sheets and observed a proper agreement between the numerical and experimental results. The HVI ballistic performance of composite multilayers of kevlar/epoxy fabrics was experimentally and numerically examined by Khodadadi et al. [14]. They simulated their numerical model in LS-DYNA software and performed experiments in the velocity range of 120-20 m/s using spherical and flat impactors. Their results show that the ballistic limit of the composite with the flat-head impactor was about 15% higher than the spherical one. Roudbeneh et al. [15] illustrated a numerical approach to simulate high-velocity impact loading in honeycomb sandwich panels reinforced with polymer foam. Torabizadeh and Fereidoon [16] experimentally analyzed composite sheets with aluminum foam core and aluminum or composite shell under the drop weight load at room temperature considering different top layers, foam core thicknesses, and impactor geometries They found that the sheets with orthogonal composite top layers could be a good alternative to conventional aluminum top layers under low-velocity impact loads. Karaglozova [17] and colleagues succeeded in presenting a finite element model for carbon/epoxy composite tubes under low-velocity axial load. They developed their numerical model based on a novel method relying on the delamination process. Two orthogonal and angular layups were studied using the shell element. The failure criteria were modeled in ABAQUS software and the numerical results were compared with the empirical data of the other authors. The mechanical and high-velocity impact performance of a hybrid long carbon/glass fiber/polypropylene thermoplastic composite was investigated by Asenjan et al. [18]. Taheri et al. [19] investigated the effect of stacking sequence on the failure mode of fiber metal laminates under low-velocity impact numerically and experimentally. They used a drop weight impact test and employed ABAQUS/explicit for the simulation of the FE model. Good agreement was reported between numerical and experimental results.

Regarding the literature review in this field, it is essential to develop a finite element-based simulation to save costs and time and offer a quick way of investigating and understanding the effect of various parameters of sandwich composite sheets on their behavior. To do this, the finite element software, ABAQUS/Explicit, was employed to simulate the drop weight impact test of foam sandwiched composite. Failure patterns of composite skin layers and Al foam core were investigated. Furthermore, in this study, a new generation of composite sandwich panels was developed by replacing AL face sheets with glass/epoxy laminated composite. This type of composite sandwich panel provides similar impact performance in comparison with existing sandwich panels with lower production cost and weight. Therefore, the ultimate objective of this

research is to develop a numerical model to assess the failure modes of sandwich composites with aluminum foam core and different top layers under low-velocity impact at room temperature... The obtained results were compared with experimental reports to evaluate the accuracy of the proposed finite element model. Then, using the proposed numerical model, the behavior of the sheets was assessed by analyzing several output components of the model, and the effect of different top layers and glass/epoxy composite top layers with cross-ply and quasi-isotropic layups were considered. Finally, while evaluating the accuracy of the numerical model, the effect of some production parameters was assessed on the final behavior of the structure.

2. Materials and Methods

A356 cast aluminum alloy was employed as the base phase, while SiC particles (purity: 98%; average particle size: 11 μm) served as the reinforcing phase. Calcium carbonate powder with (purity: 99.5%; mean size: 5 μm) was also used as a foaming agent. More details on the fabrication process and foam properties can be found in [1]. Unidirectional glass fiber fabrics were used to prepare the top layer. Each layer had a thickness of 0.2 mm and a mass of 200 g/m^2. This type of fiber is currently considered for various industrial applications. ML503 epoxy resin and HA11 hardener[1], which are commonly used in domestic industries, were utilized. The top and bottom layers had 10 layers each with different layups. The manual production of top and bottom layers at room temperature will lead to the formation of two different types of cross-ply ([0/90]) and quasi-isotropic [0/±45/90]) structures. Pure aluminum was also used for comparison. For chemical consistency, the top and bottom layers were connected to the aluminum foam core using the same two-component epoxy resin applied in the production of composite layers at a very small thickness and low clamp pressure. The dimensions of the samples were based on the fixture of the device used (120×120 mm^2, and a thickness of 20 mm) (Table 1). Figure 1 shows an example of aluminum foam next to a cross-ply sandwich composite sheet.

Table 1. Geometrical specifications of the produced specimens

Top layer	Thickness of the foam core (mm)	Thickness of the top layer (mm)	Weight of the sample (g)
Aluminum	20	2	388
Quasi-isotropic	20	2	301
Cross-ply	20	2	278

[1] Supplied by MOKARRAR Materials Engineering Company, Iran

The low-velocity impact was carried out by a drop-weight machine made by Iran Sayesh Company in the Fracture Mechanics Laboratory of the Faculty of Mechanical Engineering of K. N. Toosi University of Technology. In this apparatus, the projectile is on a rail with very little friction for free falling. In this research, the low amount of friction in the rails and equipment of the device was neglected according to the manufacturer's recommendation. The total mass of the impactor and its accessories (force sensor, bearings ...) is 7 kg, which can fall on the target from a maximum height of 1 m. The capacity of the force sensor is 10 KN and with a data collection frequency of 25 kHz. The mass and height of the impactor can be changed to reach different kinetic energies.

For all the tests, the weight of the impactor was increased to 17 kg by adding a 10-kg weight. The impactor fell on the samples from a height of 70 cm.

(a)

(b)

Fig.1. Produced specimens for impact tests (a) AL foam (b) Composite sheet with a cross-ply top layer

Figure 2 illustrates the applied apparatus. As seen, the square-shaped samples were placed on the support and fixed by 4 screws. In this way, all four edges of the sample were clamped with a width of 10 mm; leaving a 100×100 mm^2 area for the test. The spherical impactor precisely fell on the center of the sample (Fig. 2 b). All the tests were carried out based on the ASTM D7136 standard [20]. To prevent the re-collision of the impactor, a pneumatic jack was applied which operated after the first impact and stopped the impactor immediately. To prevent experimental scatter, each impact test was repeated three times. By computing statistic parameters (mean value and standard deviation), the reliability of outputs is evaluated with 90% accuracy. For more information about the experimental procedure and details, see Ref. [16].

(a)

(b)

Fig. 2. Drop-weight device (a) Overall view, (b) Collision of the weight on the sample.

3. Finite element model

The finite element method as implemented in ABAQUS/Explicit was used to simulate the impact load. To this end, a square composite sheet was studied under clamped boundary conditions according to the fixture of the applied device. ENCASTRE boundary conditions are imposed for all sides of the plate as $U_1=U_2=U_3=0$. Figure 3 depicts the finite element model of the sandwich composite sheet with a spherical impactor along with the boundary conditions. Element size is determined by convergence analysis of the FEM model of the plate. For this purpose, FEM simulations are performed with different mesh sizes and the residual kinetic energy is compared as a function of the element size. From this analysis, it can be seen that the residual kinetic energy increases with an increase in the number of elements through the thickness of the plate. However, the change in residual kinetic energy is low when the number of elements across the thickness increases from 10 to 20 (about 13%). Since the computational cost associated with 10 elements is significantly lower than with 20 elements, it is desirable to have 20 elements through the plate thickness. The top and bottom layers of the sandwich composite were modeled by a reduced linear shell element (S4R); while the AL foam core was meshed by a linear reduced solid element (C3D8R). The convergence of the applied meshes was assessed to make sure the mesh size reaches acceptable results. The top and bottom surfaces of the sandwich sheet were modeled by *SPECIAL SKIN SHELL in the software which is considered a complete connection to the foam core.

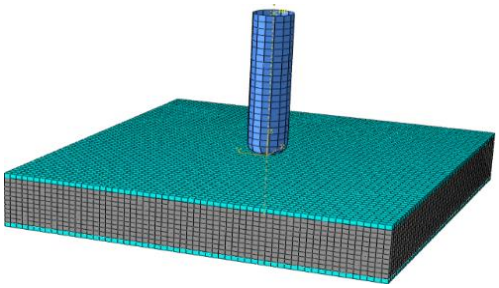

(a)

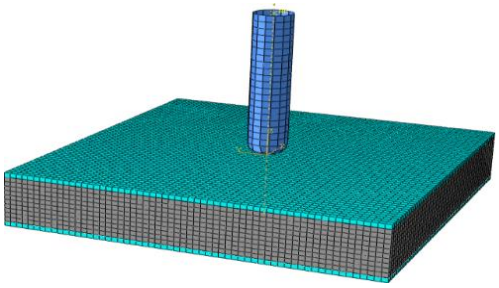

(b)

Fig. 3. (a) Finite element model of the sandwich composite sheet along with the spherical impactor (b) Clamped boundary condition in the finite element model.

The mutual effect of the sheet and impactor was simulated in two steps using ABAQUS software. Finally, the metallic impactor with a spherical head (diameter of 13 mm) was modeled as a solid object. The foam core was modeled as an elastic-plastic material. To simulate the elastic part of the matter, the isotropic elastic module was used considering the input elasticity modulus and Poisson's ratio coefficient of the AL foam. The behavior of the aluminum foam part was simulated utilizing the *CRUSHABLE FOAM and *CRUSHABE FOAM HARDENING options in the software with 0.25 g/cm^3 density, 354 MPa Young's modulus, and 1.71 compression yield stress ratio [22]. The hardening features of the foam were modeled based on the axial compressive yield strength and the stress-strain data from the empirical axial compression tests in [1]. Figure 4 shows the stress-strain diagram of the AL foam which first showed a linear behavior based on which the elasticity modulus can be determined. By further increase of the compressive load, the diagram reached a plateau (i. e. the stress remained constant by incrementing the strain) which indicates the onset of the internal destruction of the foam at yield stress. With further increase of the load and the failure of the cell walls of the foam, stress again increased in the final section of the diagram. The nonlinear finite element model was used to simulate the collision of the impactor to the sandwich sheets utilizing ABAQUS/Explicit software.

The top and bottom surfaces of the sandwich sheet were also simulated as elastic glass/epoxy material based on the experimental mechanical parameters tested by the authors (Table 2). These surfaces were defined in terms of the mechanical properties of unidirectional fibers. Figure 5 represents the layup of the cross-ply and quasi-isotropic composite surfaces.

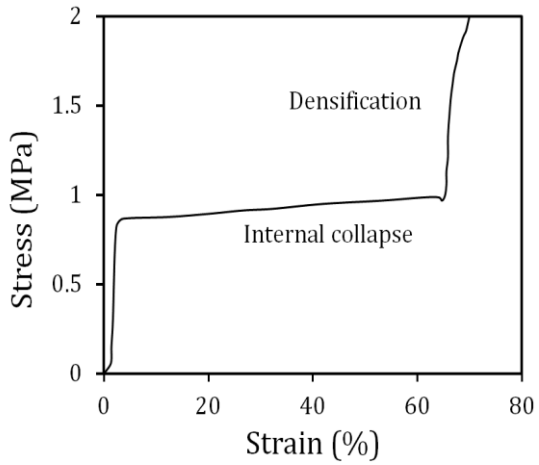

Fig. 4. Stress-strain behavior of the foam core under compressive load [1].

Table 2. Description of the properties of skin layers used [21]

Properties	Value
Longitudinal tensile modulus (GPa)	19.94
Transverse tensile modulus (GPa)	5.830
In-plane shear modulus (GPa)	2.110
Longitudinal tensile strength, (MPa)	700.1
Longitudinal compressive strength, (MPa)	570.3
Transverse tensile strength, (MPa)	69.85
Transverse compressive strength, (MPa)	122.1
In-plane shear strength, (MPa)	68.89

Hashin's failure criteria were employed to evaluate and identify the matrix and fibers failure under compression and tension (4 types of failure modes) with the following representations:

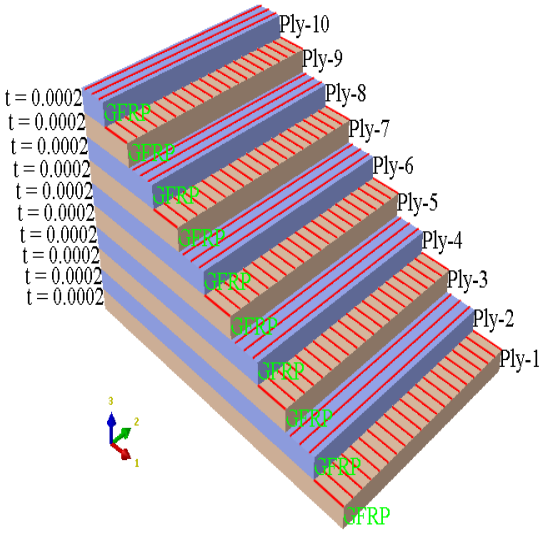

(a)

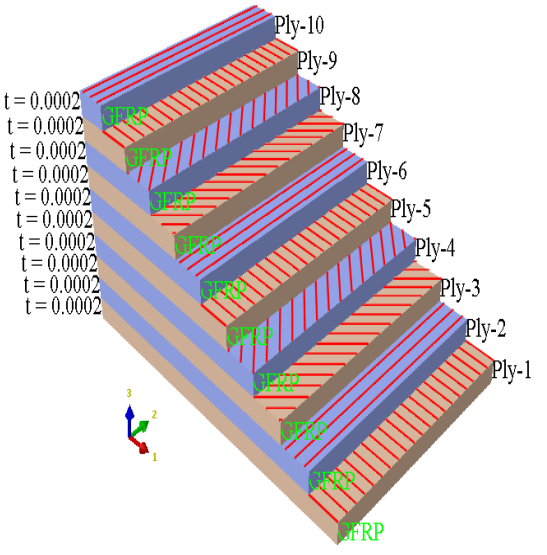

(b)

Fig. 5. Composite skin layer (a) Cross-ply (b) Quasi-isotropic used in finite element modelling

$$\left(\frac{\sigma_{11}}{X_T}\right)^2+\left(\frac{\sigma_{12}}{S}\right)^2 = e_{F+}^2 \quad \begin{cases} e_{F+}\geq 1 & failure \\ e_{F+}<1 & no\ failure \end{cases}$$ Fiber failure under tension (1)

$$\frac{\sigma_{11}}{X_C} = e_{F-} \quad \begin{cases} e_{F-}\geq 1 & failure \\ e_{F-}<1 & no\ failure \end{cases}$$ Fiber failure under compression (2)

$$\left(\frac{\sigma_{22}}{Y_T}\right)^2+\left(\frac{\sigma_{12}}{S}\right)^2 = e_{M+}^2 \quad \begin{cases} e_{M+}\geq 1 & failure \\ e_{M+}<1 & no\ failure \end{cases}$$ Matrix failure under tension (3)

$$\left(\frac{\sigma_{22}}{Y_C}\right)^2+\left(\frac{\sigma_{12}}{S}\right)^2 = e_{M-}^2 \quad \begin{cases} e_{M-}\geq 1 & failure \\ e_{M-}<1 & no\ failure \end{cases}$$ Matrix failure under compression (4)

in which, σ_{ij} shows the components of stress tensor and i and j are respectively indicative of the longitudinal and transverse directions relative to the fibers in each layer. The thickness alignment is also denoted by z. The failure criterion of Johnson-Cook which is based on nonlinear deformation was also utilized to predict the defects in the AL layer using finite element modeling as given in the following:

$$\sigma_y(\varepsilon_p,\dot{\varepsilon}_p,T) = \left[A+B(\varepsilon_p)^n\right]\left[1+\mathrm{C}\ ln(\dot{\varepsilon_p}^*)\right]\left[1-(T^*)^m\right] \quad (5)$$

The first term in the square bracket accounts for the effect of strain at the point of deformation. In this ε_p is the cumulative plastic strain, A is equal to the initial yield stress at the reference strain rate at the reference temperature, B is the hardening term and n is the exponent on the cumulative equivalent plastic strain. The second term characterizes the effect of strain rate on the deformation behavior with C as the strain rate constant and $\dot{\varepsilon_p}^*$ is a ratio of instantaneous strain rate ($\dot{\varepsilon}_p$) to reference strain rate ($\dot{\varepsilon}_0$). The effect of temperature is captured by the third term. T^* is defined as $T^* = \frac{(T-T_0)}{(T_m-T_0)}$, where T_m is the melting temperature of the metal, T_0 is the reference temperature and T is the instantaneous temperature. Constants A, B, n, m is evaluated experimentally. For more details see Ref. [22].

4. Results and discussions

The accuracy and validity of the finite element model were explored by comparing the maximum impact force, maximum displacement, and specific absorbed energy with the experimental data. Figures 6 and 7 represent the force values obtained by numerical and experimental methods for the sandwich composite sheets with cross-ply and quasi-isotropic skin layers, respectively.

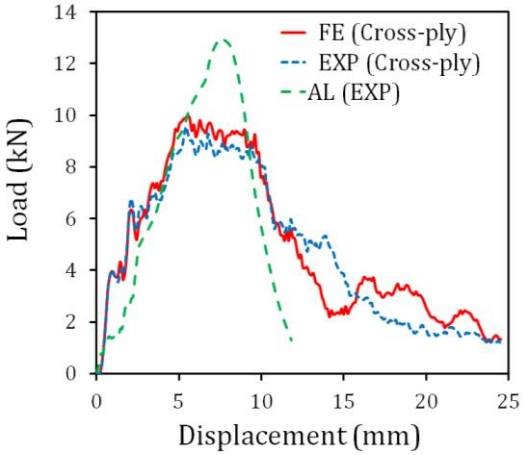

Fig. 6. Numerical and experimental force-displacement diagram of the sandwich composite sheet with cross-ply skin layer compared with the conventional AL layer

A similar diagram of the conventional AL top layer is also presented for comparison. As expected, the maximum impact force of the AL top layer was higher than the two composite skin layers. Regarding the higher weight of the samples with AL top layer, the influence of the sample weight was neutralized by comparing the specific absorbed energy which is defined as the ratio of the absorbed energy to the sample weight.

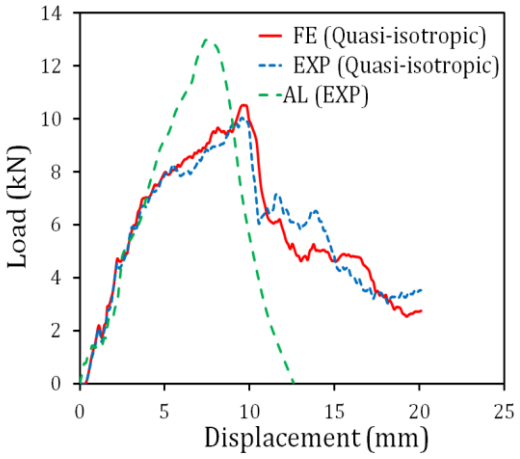

Fig. 7. Numerical and experimental force-displacement diagram of the sandwich composite sheet with quasi-isotropic skin layer compared with the conventional AL layer

The comparison results revealed a proper consistency between the results. Experimental and numerical force-displacement diagrams also exhibited similar patterns. They showed an initial linear part followed by deformation due to the sheet failure. Both empirical and numerical diagrams showed several oscillations in all cases which might be assigned to the vibrations of the support, material failure onset, or noises in the sensors. In the case of the sandwich composite sheet with a quasi-isotropic skin layer, the impactor stopped in the foam core after

destroying the top layer with no destruction in the bottom layer. For the cross-ply skin layer, however, the destruction of the bottom layer can be also observed. As the total thickness of the sample was 24 mm, this important point can be determined from the final displacement of the impactor. This phenomenon was also observed in the experimental samples. Concerning the cross-ply skin layer, after reaching the maximum force (first peak), a sudden drop, followed by a slight increment (second peak) can be observed in the force value. This behavior can be due to the destruction of the top layer at the first peak and then penetration of the impactor into the foam core and collision with the bottom layer. By increasing the kinetic energy of the sample, the second peak of the force-displacement diagram got more evident [2]. The numerical and experimental maximum impact forces of the sandwich sheets with cross-ply and quasi-isotropic skin layers can be compared in Figures 6 and 7. Numerical values are so close to the experimental finding, however, the numerical results were slightly higher than the experimental ones although the difference was acceptable. These differences can be due to the initial defects of the experimental specimens which cannot be identified in the finite element modeling. For example, non-uniform distribution of the resin, incomplete bonding of the skin layers and foam core, or different layers of composite surfaces can lead to some initial defects during the production process.

As mentioned earlier, the difference in the final displacement of the samples indicates the different penetration depths of the impactor in the three layers (top and bottom layers and foam core). The lowest and highest penetration depths of the impactor were observed in the samples with AL and cross-ply skin layers, respectively. Figure 8 illustrates the cross-section of the samples and the penetration depth of the samples with different skin layers to evaluate and validate the experimental and numerical results. The failure mode of the samples can be also determined. Since the analysis of specimen damage and its mechanism of destruction was not the subject of this article, it is merely a case report. As can be seen, the spherical impactor entered the plate with aluminum and quasi-isotropic surfaces from the top but stopped in the foam core of the plate while for the cross-ply skin layer, the impactor passes through the bottom plate. The separation of the skin layer was observed in the case of the cross-ply sample, which was not seen in the quasi-isotropic case. Also, the maximum penetration was observed in the plate with a cross-ply skin layer while the lowest one was detected in the plate with a pure aluminum surface. As seen, fiber failure and delamination of the surface layer from the foam core, as well as matrix cracking, are among the main failure modes which are in proper agreement with the prediction of the finite element modeling based on Hashin's failure criterion. Furthermore, the results of Figs. 6 and 7 on the impactor penetration can be observed in Fig. 8 as well.

Figure 9 depicts the top face of the sandwich composite sheets with AL, quasi-isotropic, and cross-ply skin layers after impact with the spherical impactor and compares them with the numerical values. Noteworthy, the finite element results of this figure are related to the main failure in the sandwich sheets in all layers and elements of the model. To illustrate the failure in the sample with the AL skin layer, the output of the Johnson-Cook criterion was presented. For a better comparison of the results, the visible defect areas of the experimental samples are marked by red color. As seen, the area and pattern of the failure presented by the numerical finite element method showed proper consistency with the experimental findings.

Based on Hashin's failure criteria, each layer has a different mode of failure. For example, for the cross-ply skin layer, the fiber failure under tension criterion (right pattern), and also the fiber failure under compression criterion (left pattern), are separately shown in Fig.10. As can be seen, these failure modes gradually decreased with the passing of the impactor through the top layer and reaching other layers. However, in the last few layers of the cross-ply skin layer, due to the incomplete bonding with the foam core and the consequent increase in the delamination of layers, the amount of damage increased again.

The energy absorbed due to the deformation of the sandwich composite sheet can be obtained by calculating the area under the force-displacement diagram. Since the sample weight is one of the effective parameters in the absorbed energy, as mentioned earlier, the effect of sample weight was eliminated by considering the concept of specific absorbed energy. Figure 11 shows the specific absorbed energy of the sandwich composite sheets with different skin layers. This quantity showed proper agreement with the numerical results in the case of the aluminum surface due to the formation of fewer structural defects during production. However, in samples with the composite surface, due to the greater sensitivity in the production process and the greater probability of initial defects, a larger difference can be observed between the experimental and numerical results. The highest specific absorbed energy belongs to the sandwich sample with a quasi-isotropic skin layer while the lowest one was detected in the sample with the aluminum skin layer. The sample with quasi-

isotropic layers exhibited higher impact resistance and as a result, more flexibility (ability to absorb kinetic energy) due to the presence of ± 45 layers as reported in [2].

The stress is transferred from the upper layer of the sandwich sheet to the foam core and then to the bottom layer. The stress distribution depends on its density and elasticity modulus, and the time it takes to pass through the layers. Three nodes from three different positions of the finite element model of the sandwich sheet with the cross-ply composite surface (top and bottom faces as well as the core) were selected and the history of the stress distribution was investigated as depicted in Fig. 12. The results indicated that the highest stress was in the top and bottom layers, whereas the foam core exhibited the lowest stress.

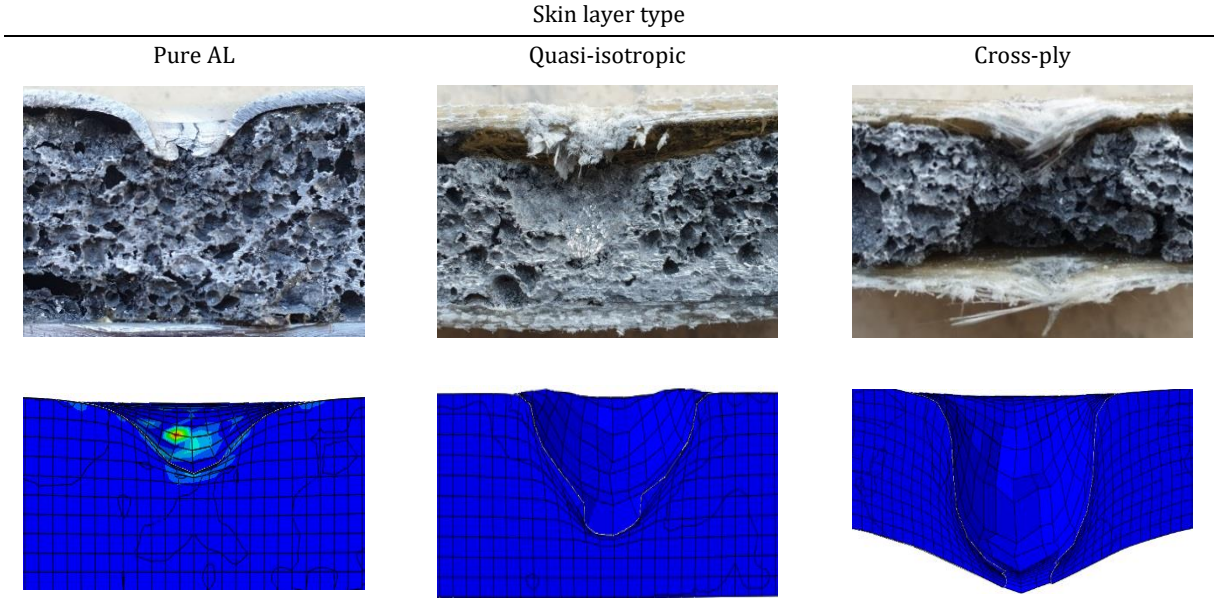

Fig. 8. A cross-section of the sandwich composite sheet with cross-ply, quasi-isotropic, and AL skin layers obtained by numerical and experimental results.

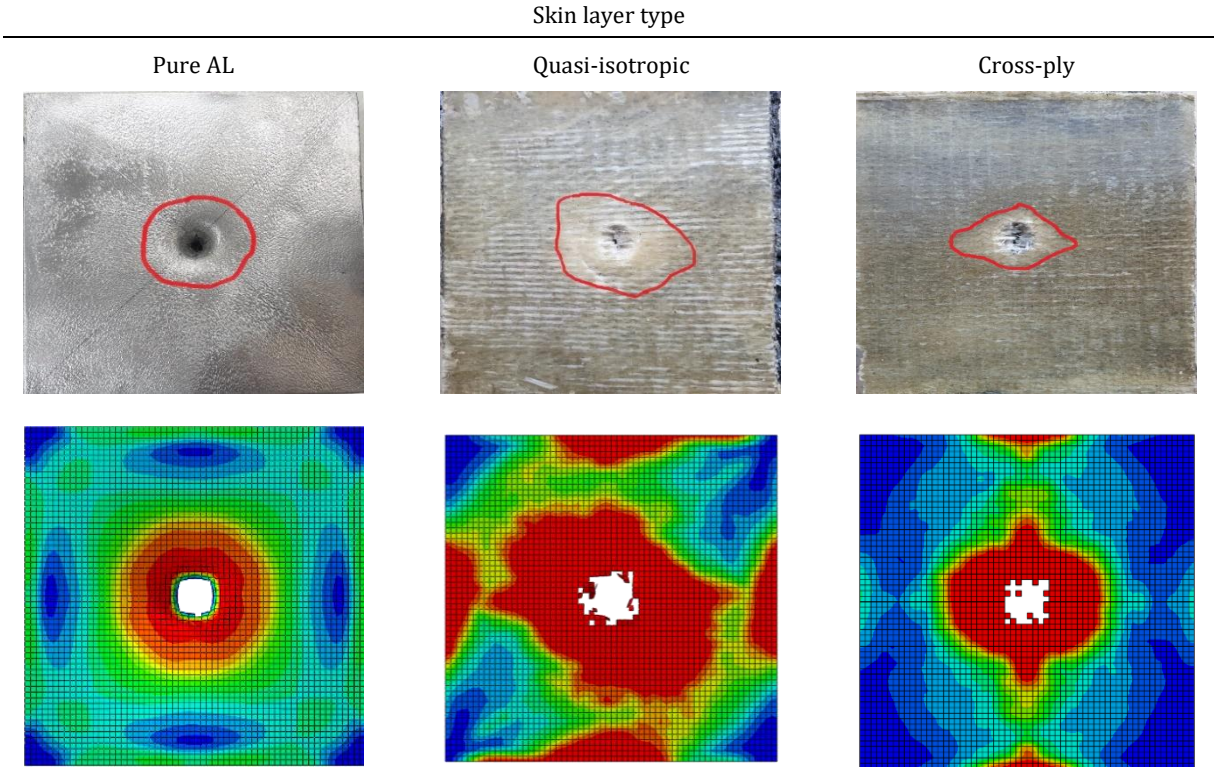

Fig. 9. The top layer of the sandwich composite sheet with AL, quasi-isotropic, and cross-ply top layers obtained by experimental and numerical analysis

The reason could be searched in the low elasticity modulus and density of the AL foam compared to the mechanical properties of the composite skin layer. The first stress peak can be seen at t=0.0016 s which is the time of the destruction of the cross-ply composite top layer. Regarding the low thickness of this layer, the stress distribution was immediately extended to the foam core. Then, the first stress peak in the bottom layer was observed at t=0.005 s with a relatively long-time distance from the top layer, indicating that the impactor required 0.0034 s to pass the foam core. Such a long time can be assigned to the low density and high thickness of the AL foam.

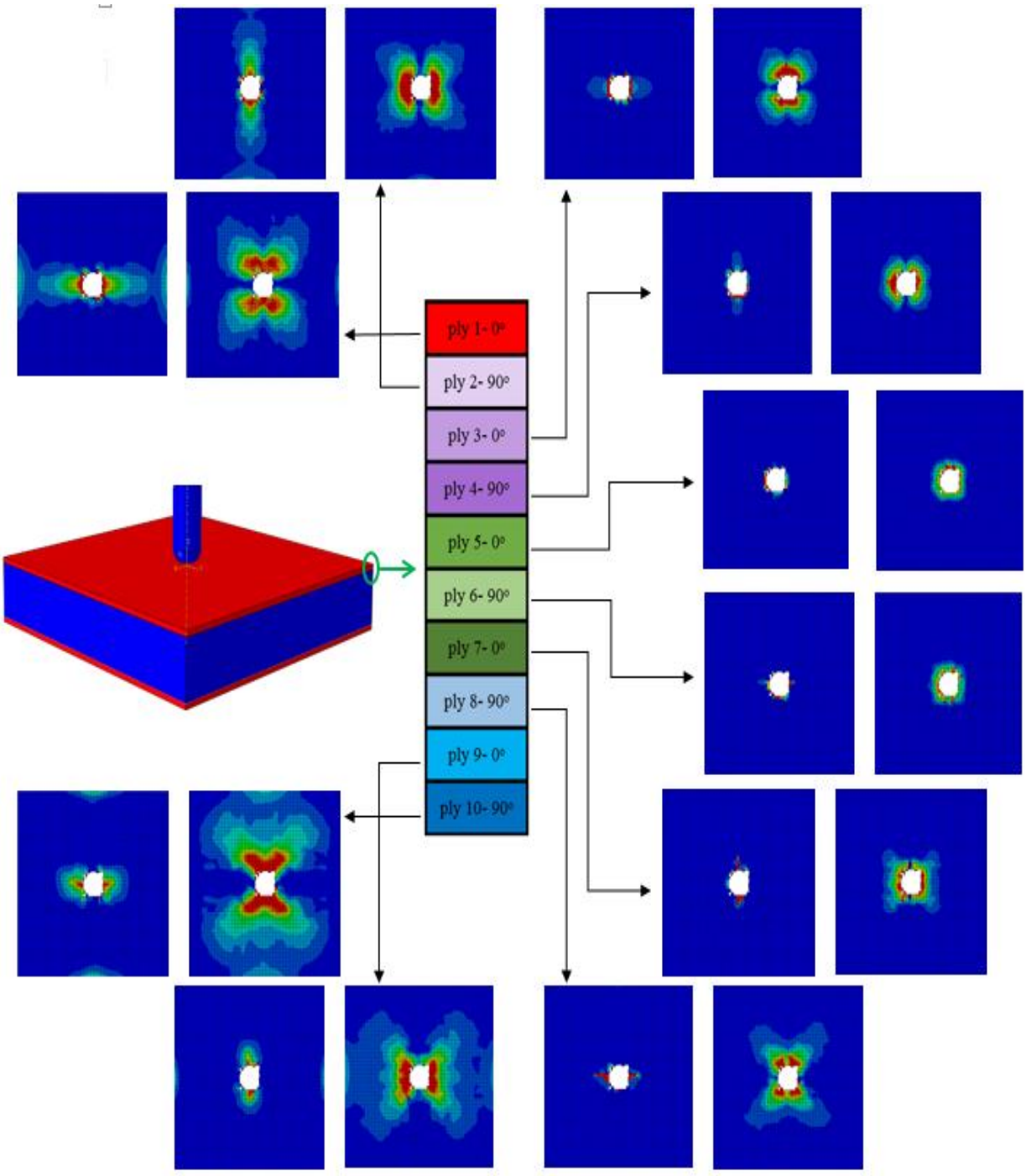

Fig. 10. Failure of the sandwich composite sheet with cross-ply skin layer considering the fiber failure in tension (right) and fiber failure under compression (left) for each layer.

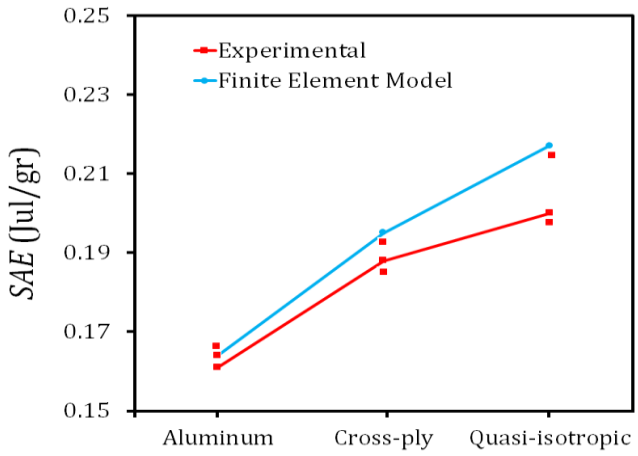

Fig. 11. Numerical and experimental specific absorbed energy of the sandwich composite sheets with various skin layers

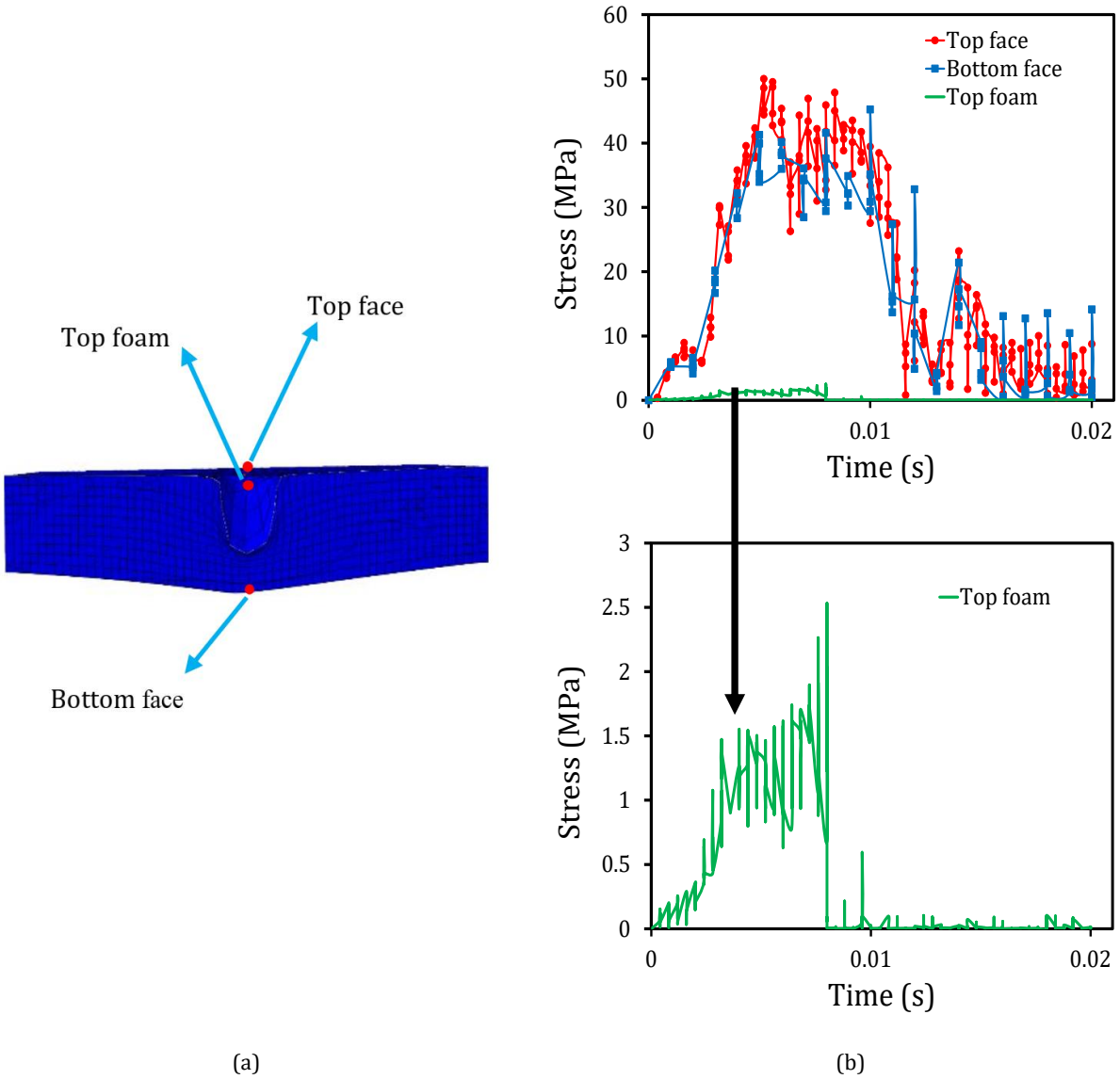

Fig. 12. (a) Three points selected on the top layer, foam core, and bottom layer (b) History of stress distribution in the composite sheet with cross-ply skin layer

5. Conclusion

The behavior and properties of sandwich composite sheets with various skin layers (AL, cross-ply, and quasi-isotropic) were numerically and experimentally explored under low-velocity impact. A comparison between the specific absorbed energy, force displacement, and failure pattern indicated a proper agreement between the experimental and numerical findings. Both methods showed similar destruction behavior. However, in the numerical model, debonding between surfaces and foam core and delamination of composite layers could be neglected. Moreover, in numerical results, the destruction area indicated more symmetry compared to the experimental ones. The type of the face sheets and the fiber alignment in the composite surfaces significantly affected the impact behavior such as maximum impact force, failure mode, and absorbed energy. Based on the comparisons, the composite sheets with a quasi-isotropic skin layer had the highest specific absorbed energy; thus, it could be a proper alternative for the conventional AL surfaces of the sandwich sheets with foam core.

Conflicts of Interest

The author declares that there is no conflict of interest regarding the publication of this manuscript. In addition, the authors have entirely observed the ethical issues, including plagiarism, informed consent, misconduct, data fabrication and/or falsification, double publication and/or submission, and redundancy.

References

[1] Torabizadeh, M.A., 2021. Experimental study of the effect of impact shape and skin layout on the behavior of aluminum foam core sandwich panels at low-velocity impact load. In Persian, *Journal of Science and Technology of Composi*tes, 7, pp.1153-1162.

[2] Mohmmed, R., Zhang, F., Sun, B. and Gu, B., 2013. Finite element analyses of low-velocity impact damage of foam sandwiched composites with different ply angles face sheets. *Materials and Design*, 47, pp.189–199.

[3] Bozkurt, M.O., Parnas, L. and Coker, D., 2019. Simulation of Drop-Weight Impact Test on Composite Laminates using Finite Element Method. *Procedia Structural Integrity*, 21, pp.206-214.

[4] Sun, M., Chang, M., Wang, Z., Li, H. and Sun, X., 2018. Experimental and Simulation Study of Low-Velocity Impact on Glass Fiber Composite Laminates with Reinforcing Shape Memory Alloys at Different Layer Positions. *Applied Sciences*, 8, pp.1-15.

[5] Riccio, A., Di Felice, G., Saputo, S. and Scaramuzzino, F., 2014. Stacking Sequence Effects on Damage Onset in Composite Laminate Subjected to Low Velocity Impact. *Procedia Engineering*, 88, pp.222-229.

[6] Guo, Z., Li, Z., Zhu, H., Cui, H., Li, D., Li, Y. and Luan, Y., 2020. Numerical simulation of bolted joint composite laminates under low velocity impact. *Materials Today Communications*, 23, pp.1-8.

[7] Soydan, A., Tunaboylu, B., Galal Elsabagh, A., Kadir Sarı, A. and Akdeniz, R., 2018. Simulation and Experimental Tests of Ballistic Impact on Composite Laminate Armor. *Advances in Materials Science and Engineering*, 11, pp.1-12.

[8] Ahmad, A., Abbassi, F., Kyun Park, M., Jung, J. and Hong, J., 2018. Finite element analysis for the evaluation of the low-velocity impact response of a composite plate. *Advanced Composite Materials*, 28, pp.1-15.

[9] Wang, N., Chen, Z., Li, A., Li, Y., Zhang, H. and Liu, Y., 2016. Three-point bending performance of a new aluminum foam composite structure. *Transactions of Nonferrous Metals Society of China*, 26, pp.359-368.

[10] Liu, T., Zhang, X., He, N. and Jia, G., 2017. Numerical Material Model for Composite Laminates in High–Velocity Impact Simulation. *Latin American Journal of Solids and Structures*, 14, pp.1590-1679.

[11] Cui, H., Thomson, D., Eskandari, S. and Petrinic, N., 2019. A critical study on impact damage simulation of IM7/8552 composite laminate plate. *International Journal of Impact Engineering*, 127, pp.100-109.

[12] Subramani, K. and Vinoth kanna, I., 2018. Numerical Simulation of High Velocity Impact on Composite Targets Using Advanced Computational Techniques. In *Lecture Notes in Mechanical Engineering*. (IDAD 2018), pp.399-413.

[13] Safarabadi, M. Ashkani, P. and Ganjiani, S.M., 2018. Finite element simulation of high velocity impact on polymer composite plates. In Persian, *Journal of Science and Technology of Composites*, 5, pp.157-168.

[14] Khodadadi, A., Liaghat, Gh., Ahmadi, H., Bahramian, A., Shahgholian-Ghahfarokhi, D., Anani, Y., Asemani, S.S., 2019. Experimental and numerical analysis of high velocity impact on Kevlar/Epoxy composite plates. In Persian, *Journal of Science and Technology of Composites*, 6, pp.265-274.

[15] Roudbeneh F, Liaghat Gh, Sabouri H, Hadavinia H., 2020. High-velocity impact loading in honeycomb sandwich panels

reinforced with polymer foam: a numerical approach study. *Iran Polym Journal*, 29, pp.707-721.

[16] Torabizadeh, M.A., Fereidoon, A., 2021. Applying Taguchi Approach to Design Optimized Effective Parameters of Aluminum Foam Sandwich Panels under Low-Velocity Impact. *Iranian Journal Science and Technology, Transactions of Mechanical Engineering*, https://doi.org/10.1007/s40997-021-00441-5.

[17] Karaglozova, D., Ataabadi, P. and Alves, M., 2021. Finite Element Modeling of CFRP composite tubes under low velocity axial impact. *Polymer Composites*, 42, pp.1543-1564.

[18] Asenjan M, Sabet SA, Nekoomanesh M., 2020. Mechanical and high velocity impact performance of a hybrid long carbon/glass fiber/polypropylene thermoplastic composite. *Iran Polym Journal*. Published Online.

[19] Taher-Behrooz F, Shokrieh MM, Yahyapour I., 2013. Effect of stacking sequence on failure mode of fiber metal laminates under low-velocity impact. *Iran Polym Journal*, 23, pp.147-152.

[20] ASTM D7136, 2020. Standard Test Method for Measuring the Damage Resistance of a Fiber-Reinforced Polymer Matrix Composite to a Drop-Weight Impact Event.

[21] Shokrieh MM, Torabizadeh MA, Fereidoon A., 2012. A new method for evaluation of mechanical properties of glass/epoxy composites at low temperatures. *Strength of Materials,* 44, pp.87-99.

[22] Golestanipur M, Doorandish S, Tadayoni S, Babakhani A, Zebarjad M, Naderi B., 2014. Investigation of deformation of sandwich panel with aluminum foam core under projectile fall test. *Advanced Proceeding in Materials Engineering,* 9, pp.11-23.